Available online at www.sciencedirect.com

Integrative Medicine Research

journal homepage: www.imr-journal.com

Original Article

Induction of apoptosis by Dae-Hwang-Mok-Dan-Tang in HCT-116 colon cancer cells through activation of caspases and inactivation of the phosphatidylinositol 3-kinase/Akt signaling

Cheol Park[a], *Su Hyun Hong*[b], *Yung Hyun Choi*[b,c,*]

[a] *Department of Molecular Biology, College of Natural Sciences, Dongeui University, Busan, Korea*
[b] *Department of Biochemistry, Dongeui University College of Korean Medicine, Busan, Korea*
[c] *Anti-Aging Research Center & Blue-Bio Industry Regional Innovation Center, Dongeui University, Busan, Korea*

ARTICLE INFO

Article history:
Received 10 January 2017
Accepted 21 March 2017
Available online 26 May 2017

Keywords:
apoptosis
caspase
Dae-Hwang-Mok-Dan-Tang
HCT-116 cells
PI3K/Akt

ABSTRACT

Background: Dae-Hwang-Mok-Dan-Tang (DHMDT), a traditional Korean medicine, contains five species of medicinal plants and has been used to treat patients with digestive tract cancer for hundreds of years; however, its anticancer mechanism is poorly understood. In the present study, we investigated the proapoptotic effects of DHMDT in human colon cancer HCT-116 cells.

Methods: Cytotoxicity was evaluated using the 3-(4,5-dimethyl-2-thiazolyl)-2,5-diphenyl-2*H*-tetrazolium bromide assay. Apoptosis was detected using 4,6-diamidino-2-phenyllindile staining, agarose gel electrophoresis, and flow cytometry. The protein levels were determined using Western blot analysis. Caspase activity was measured using a colorimetric assay.

Results: Treatment with DHMDT resulted in a growth inhibition coupled with apoptosis induction, which was associated with the downregulation of members of IAP (inhibitor of apoptosis protein) family, including XIAP and survivin, and the activation of caspase-9 and -3 accompanied by proteolytic degradation of poly(ADP-ribose)-polymerase and phospholipase C-γ1. DHMDT treatment also showed a correlation with the translocation of proapoptotic Bax to mitochondria, the loss of mitochondrial membrane permeabilization, and the cytochrome c release from the mitochondria to the cytosol. Moreover, DHMDT increased the levels of death receptor-associated ligands and enhanced activation of caspase-8 and cleavage of its substrate, Bid. However, the pan-caspase inhibitor could reverse DHMDT-induced apoptosis. In addition, DHMDT suppressed the phosphoinositide 3-kinase (PI3K)/Akt pathway, and treatment with a potent inhibitor of PI3K further increased the apoptotic activity of DHMDT.

* *Corresponding author*. Department of Biochemistry, Dongeui University College of Korean Medicine, 52-57 Yangjeong-ro, Busanjin-gu, Busan 47227, Republic of Korea.
E-mail address: choiyh@deu.ac.kr (Y.H. Choi).

http://dx.doi.org/10.1016/j.imr.2017.03.003

Conclusion: Our data showed that DHMDT induces HCT-116 cell apoptosis by activating intrinsic and extrinsic apoptosis pathways and by suppressing the PI3K/Akt signal pathway; however, further studies are needed to identify the active compounds.

1. Introduction

Colorectal cancer is the third most common malignant cancer in men; it is also the second most common form of cancer in women and the second most common type of life-threatening cancer worldwide.1 The major methods for the treatment of cancer include surgery, chemotherapy, radiation therapy, and palliative care.2 Among them, chemotherapy is widely used to control tumor growth or to relieve symptoms after surgery.3 However, treatment with the majority of current chemotherapeutic agents is generally associated with severe side effects including cardiotoxicity, hepatotoxicity, neurotoxicity, immunosuppression, and myelosuppression.4–6 Hence, the identification of more effective and/or less toxic anticancer agents would improve the management of colorectal cancer.

The progression of cancer is characteristically linked to resistance to apoptosis, an active process of programmed cell death. Apoptosis has been characterized as a fundamental cellular activity that maintains the physiological balance of the organism.7,8 Accumulating evidence has demonstrated that the induction of apoptosis in tumor cells has been shown to be the most common anticancer mechanism conjoint with many cancer therapies. In general, apoptosis may be initiated through two major pathways: the extrinsic [death receptor (DR)-mediated] pathway and the intrinsic (mitochondrial-mediated) pathway that involves the activation of caspases.9,10 The products of several genes have been demonstrated to be critical in the regulation of these two pathways, including caspase cascades, Bcl-2, and inhibitor of apoptosis protein (IAP) family members. In the extrinsic pathway, the binding of extracellular death ligands to their cell-surface DRs leads to the activation of caspase-8. By contrast, the intrinsic pathway is activated by the release of proapoptotic factors, such as cytochrome *c* from the mitochondria to the cytosol, following loss of inner mitochondrial membrane integrity and activation of caspase-9. Moreover, the extrinsic pathway can crosstalk to the intrinsic pathway through the caspase-8-mediated cleavage of Bid, a member of the Bcl-2 family of proteins, which ultimately amplify the intrinsic apoptotic pathway.11,12 Therefore, agents that target the apoptosis pathway without affecting normal cells play crucial roles as potential drug targets in cancer treatment.

For thousands of years, herbal medicines have been used with apparent safety and efficacy for alleviating and treating various diseases in Asia, including Korea, China, and Japan. Typical traditional Korean medicinal prescriptions consist of more than four components that are mixed to minimize side effects, maximize medical effects, and improve quality of life. Among them, Dae-Hwang-Mok-Dan-Tang (DHMDT) is an aqueous polyherbal formulation, which consists of crude ingredients extracted from five herbs, that has been known to exert antidiarrhea and anti-inflammatory activities. DHMDT has been used to treat patients with digestive tract cancers in traditional Korean medicine.13 However, despite its valuable clinical effects for patients, little is known about the molecular biochemical basis of the effects of DHMDT. As a part of our search for novel biologically active substances for the prevention and treatment of cancers from traditional medicinal resources, we evaluated whether DHMDT could inhibit the growth of and trigger apoptosis in human colon cancer HCT-116 cells.

Table 1 – Components of Dae-Hwang-Mok-Dan-Tang (DHMDT) extract granules.

Herbal medicine (pharmacognostic nomenclature)	Raw material amount (g/%)
Paeonia suffruticosa ANDR (Moutan Cortex)	10.0 (23.8)
Prunus persica L. BATSCH (Persicae Semen)	10.0 (23.8)
Trichosanthes kirilowii MAXIM (Trichosanthis Fructus)	10.0 (23.8)
Rheum plamatum L. (Rhei Radix)	6.0 (14.3)
Mirabilite (Natrii Sulfas)	6.0 (14.3)
Total amounts	42 (100)

2. Materials

2.1. Preparation of the DHMDT extract

DHMDT, which is composed of five medicinal plants (Table 1), was obtained from Dongeui Oriental Hospital, Dongeui University College of Oriental Medicine (Busan, Republic of Korea). Each of the five herbs in DHMDT was cut into small pieces and then mixed together to obtain a total amount of 42 g in the ratios shown Table 1. The mixture was boiled with distilled water (42 g/500 mL) for 3 hours. The extract was filtered with a 0.45-mM filter to remove insoluble materials, and the filtrate was lyophilized and then crushed into a thin powder. The extracts were dissolved to a 100 mg/mL concentration with distilled water, and the stock solution was then diluted with medium to the desired concentration prior to use.

2.2. Cell culture and cell viability assay

The colon cancer HCT-116 cell and Chang liver (an immortalized nontumor cell line derived from normal liver tissue) cell lines were obtained from the American Type Culture Collection (Manassas, VA, USA) and maintained at 37 °C in 5% CO_2 in Dulbecco's modified Eagle's medium (Gibco-BRL, Gaithersburg, MD, USA) supplemented with 10% fetal bovine serum, and 1% penicillin/streptomycin (Gibco-BRL). The cell viability assay was performed using the 3-(4,5-dimethyl-2-

thiazolyl)-2,5-diphenyl-2*H*-tetrazolium bromide (MTT) assay. In brief, the cells were treated with different concentrations of DHMDT. After treatments for the indicated times, 0.5 mg/mL of MTT (Sigma-Aldrich Chemicals, St. Louis, MO, USA) solution was added, followed by incubation for 2 hours at 37 °C in the dark; then, the medium was removed. The formazan precipitate was dissolved in dimethyl sulfoxide (Sigma-Aldrich). Absorbance of the formazan product was measured at 540 nm with an enzyme-linked immunosorbent assay reader (Molecular Devices, Sunnyvale, CA, USA). *N*-Benzyloxycarbonyl-Val-Ala-Asp-fluoromethylketone (z-VAD-fmk), a pan-caspase inhibitor, and LY294002, a selective inhibitor of phosphatidylinositol 3-kinase (PI3K), were obtained from Calbiochem (San Diego, CA, USA) and Cell Signaling Technology, Inc. (Danvers, MA, USA), respectively. For the morphological study, the cells were photographed directly using an inverted microscope (Carl Zeiss, Oberkochen, Germany).

2.3. *Nuclear staining with 4,6-diamidino-2-phenyllindile*

For the assessment of apoptosis, the cells were washed with phosphate-buffered saline (PBS) and fixed with 3.7% paraformaldehyde (Sigma-Aldrich) in PBS for 10 minutes at room temperature. The fixed cells were washed with PBS and stained with 2.5 μg/mL of 4,6-diamidino-2-phenyllindile (Sigma-Aldrich) solution for 10 minutes at room temperature. The cells were washed twice with PBS, and the stained nuclei were analyzed using a fluorescence microscope (Carl Zeiss).

2.4. *Agarose gel electrophoresis for DNA fragmentation assay*

After DHMDT treatment, the cells were lysed in a buffer containing 10 mM Tris–HCl, pH 7.4, 150 mM NaCl, 5 mM trypsine-ethylene diamine tetraacetic acid (EDTA), and 0.5% Triton X-100 for 1 hour on ice. The lysates were vortexed and cleared by centrifugation at 19,000 *g* for 30 minutes at 4 °C. An equal volume of neutral phenol/chloroform/isoamyl alcohol (25:24:1, v/v/v; Sigma-Aldrich) was used for DNA extraction in the supernatant, followed by electrophoretic analysis on 1.5% agarose gels containing 0.1 μg/mL ethidium bromide (EtBr; Sigma-Aldrich). The DNA size marker (100 bp ladder) was purchased from Bioneer Corp. (Daejeon, Republic of Korea).

2.5. *DNA flow cytometric detection of apoptosis*

After treatment with DHMDT, the cells were harvested, washed twice with ice-cold PBS, and fixed with 75% ethanol at 4 °C for 30 min; the DNA content of the cells was stained using a DNA staining kit (CycleTEST PLUS Kit; Becton Dickinson, San Jose, CA, USA) with propidium iodide (PI). The DNA content at the sub-G1 phases was then determined using a FACSCalibur flow cytometer and analyzed using Cell Quest software (Becton Dickinson). Each of the cell samples were also stained with 5 μL annexin V-fluorescein isothiocyanate (FITC; R&D Systems, Minneapolis, MN, USA), and 5 μL PI. After incubation for 15 minutes at room temperature in the dark, the degree of apoptosis was quantified as a percentage of the annexin V-positive and PI-negative (annexin V^+/PI^- cells) cells by a flow cytometer.[14]

2.6. *Protein extraction and Western blot analysis*

The cells were harvested and lysed with lysis buffer (20 mM sucrose, 1 mM EDTA, 20 μM Tris-Cl, pH 7.2, 1 mM dithiothreitol, 10 mM KCl, 1.5 mM $MgCl_2$, 5 μg/mL pepstatin A, 10 μg/mL leupeptin, and 2 μg/mL aprotinin) for 30 minutes at 4 °C. In a parallel experiment, the mitochondrial and cytosolic fractions were isolated using a mitochondrial fractionation kit (Active Motif, Carlsbad, CA, USA) according to the manufacturer's instructions. A Bio-Rad protein assay (Bio-Rad, Hercules, CA, USA) was used according to the manufacturer's instructions to determine the protein concentrations. After normalization, an equal amount of protein was subjected to electrophoresis on sodium dodecyl sulfate-polyacrylamide gel and then transferred to a nitrocellulose membrane (Schleicher & Schuell, Keene, NH, USA) by electroblotting. The membranes were soaked in 5% skim milk and incubated with the primary antibodies and the horseradish peroxidase-conjugated antimouse or antirabbit secondary antibodies. An enhanced chemiluminescence (ECL; Amersham Corp., Arlington Heights, IL, USA) detection system was used to visualize the target proteins. The primary antibodies (Table 2) were purchased from Santa Cruz Biotechnology, Inc. (Santa Cruz, CA, USA) and Cell Signaling Technology, Inc. (Beverly, MA, USA). The peroxidase-labeled donkey antirabbit and sheep antimouse immunoglobulin were purchased from Amersham Corp.

2.7. *In vitro caspase activity assay*

The activities of the caspases were determined using colorimetric assay kits (R&D Systems), which utilize synthetic tetrapeptides [Asp-Glu-Val-Asp (DEAD) for caspase-3; Ile-Glu-Thr-Asp (IETD) for caspase-8; and Leu-Glu-His-Asp (LEHD) for caspase-9] labeled with *p*-nitroaniline (pNA) that is linked to the end of the caspase-specific substrate. Briefly, the DHMDT-treated cells and the untreated cells were lysed in the supplied lysis buffer. The supernatants were collected and incubated with the supplied reaction buffer containing dithiothreitol and DEAD-pNA, IETD-pNA, or LEHD-pNA as substrates at 37 °C for 2 hours in the dark. The reactions were measured by changes in absorbance at 405 nm using an enzyme-linked immunosorbent assay reader.

2.8. *Measurement of mitochondrial membrane potential ($\Delta\psi m$)*

The mitochondrial membrane potential (MMP) values were determined using the dual-emission potential-sensitive probe, 5,5′,6,6′-tetrachloro-1,1′,3,3′-tetraethylimidacarbocyanine iodide (JC-1; Sigma-Aldrich), which is internalized and concentrated by respiring mitochondria and, therefore, can reflect MMP changes in live cells. Briefly, the cells were collected and incubated with 10 μM of JC-1 for 30 minutes at 37 °C in the dark. After JC-1 was removed, the cells were washed with PBS to remove unbound dye, and

Table 2 – List of antibodies used in the present study.

Antibody	Dilution	Cat. No.	Species of origin and supplier
TRAIL	1:1000	sc-7877	Rabbit polyclonal, Santa Cruz Biotechnology, Inc.
DR4	1:500	sc-7863	Rabbit polyclonal, Santa Cruz Biotechnology, Inc.
DR5	1:500	sc-65314	Mouse monoclonal, Santa Cruz Biotechnology, Inc.
Fas	1:1000	sc-715	Rabbit polyclonal, Santa Cruz Biotechnology, Inc.
FasL	1:1000	sc-957	Rabbit polyclonal, Santa Cruz Biotechnology, Inc.
XIAP	1:1000	sc-11426	Rabbit polyclonal, Santa Cruz Biotechnology, Inc.
cIAP-1	1:1000	sc-7943	Rabbit polyclonal, Santa Cruz Biotechnology, Inc.
cIAP-2	1:1000	sc-7944	Rabbit polyclonal, Santa Cruz Biotechnology, Inc.
Survivin	1:500	sc-17779	Mouse monoclonal, Santa Cruz Biotechnology, Inc.
Caspase-3	1:1000	sc-7272	Mouse monoclonal, Santa Cruz Biotechnology, Inc.
Caspase-8	1:1000	sc-7890	Rabbit polyclonal, Santa Cruz Biotechnology, Inc.
Caspase-9	1:1000	sc-7885	Rabbit polyclonal, Santa Cruz Biotechnology, Inc.
PARP	1:1000	sc-7150	Rabbit polyclonal, Santa Cruz Biotechnology, Inc.
PLC-γ1	1:1000	sc-7290	Mouse monoclonal, Santa Cruz Biotechnology, Inc.
Bcl-2	1:1000	sc-509	Mouse monoclonal, Santa Cruz Biotechnology, Inc.
Bax	1:1000	sc-493	Rabbit polyclonal, Santa Cruz Biotechnology, Inc.
Bid	1:1000	sc-11423	Rabbit polyclonal, Santa Cruz Biotechnology, Inc.
PI3K	1:1000	4257	Rabbit polyclonal, Cell Signaling Technology, Inc.
p-PI3K	1:500	4228	Rabbit polyclonal, Cell Signaling Technology, Inc.
Akt	1:1000	sc-8312	Rabbit polyclonal, Santa Cruz Biotechnology, Inc.
p-Akt	1:500	9271	Rabbit polyclonal, Cell Signaling Technology, Inc.
Actin	1:1000	sc-47778	Mouse monoclonal, Santa Cruz Biotechnology, Inc.

DR, death receptor; EtBr, ethidium bromide; FasL, Fas ligand; PARP, poly(ADP-ribose)-polymerase; PI3K, phosphatidylinositol 3-kinase; PLC-γ1, phospholipase C-γ1; TRAIL, tumor necrosis factor-related apoptosis-inducing ligand.

the amount of JC-1 retained by 10,000 cells per sample was measured at 488 nm and 575 nm using a flow cytometer.

2.9. *Statistical analysis*

The data are reported as the mean ± standard deviation of three independent experiments. A one-way analysis of variance was performed to determine statistical significance. Significant differences were established at $p < 0.05$.

3. Results

3.1. *DHMDT inhibited cell viability in HCT-116 cells*

To investigate the effects of DHMDT on HCT-116 cell growth, the cells were treated with various concentrations of DHMDT, and the MTT assay was carried out after incubation for the indicated times. As shown in Fig. 1A, DHMDT inhibited the cell viability of HCT-116 cells in a concentration- and time-dependent manner. For example, the cell viability was inhibited by more than 47% or 68% in the cells exposed to 0.8 mg/mL or 1.0 mg/mL of DHMDT for 72 hours, respectively, as compared to the untreated controls. In addition, visual inspection using inverted microscopy revealed that treatment with DHMDT resulted in numerous morphological changes, including extensive cytosolic vacuolization and the appearance of irregular cell membrane buds (Fig. 1B). The results of an additional experiment using Chang liver cells, conducted to examine the effect of DHMDT on the proliferation of normal cells, are shown in Fig. 1C. The MTT assay results indicated that DHMDT concentrations up to 1.0 mg/mL did not induce cytotoxicity. Therefore, the highest concentration of DHMDT in HCT-116 colon cancer cells was selected as 1 mg/mL.

3.2. *DHMDT induced apoptosis in HCT-116 cells*

To answer the question of whether growth inhibition by DHMDT was associated with the induction of apoptosis, we examined apoptotic features by measuring the chromatin condensation of the nuclei, DNA fragmentation, and the amount of sub-G1 phase and annexin V-positive cells. As shown in Fig. 2A, treatment with DHMDT resulted in the observation of a significant number of cells with chromatin condensation and the formation of apoptotic bodies in a concentration-dependent manner, whereas these features were not observed in the control cells. Treatment with DHMDT induced progressive accumulation of fragmented DNA, which appeared as a typical ladder pattern of DNA fragmentation in a concentration-dependent manner (Fig. 2B). In addition, treatment with DHMDT resulted in the increased accumulation of cells in the apoptotic hypodiploid sub-G1 phase and an increase in the number of annexin V-positive cells (Fig. 2C and D). Taken together, these results revealed that the cytotoxic effects observed in response to DHMDT are associated with the induction of apoptosis in HCT-116 cells.

3.3. *DHMDT modulated the expression of apoptosis-related genes in HCT-116 cells*

In order to determine which apoptosis pathway contributes to DHMDT-induced apoptosis, the levels of DR and corresponding proapoptotic ligands were first examined by Western blot analyses. After DHMDT treatment, the protein levels of DR4, DR5, and Fas were not altered; however, the expression of tumor necrosis factor (TNF)-related apoptosis-inducing ligand (TRAIL) and Fas ligand (FasL) increased in a concentration-dependent manner (Fig. 3). Next, we examined the effects of DHMDT on the levels of the IAP family proteins. The results of

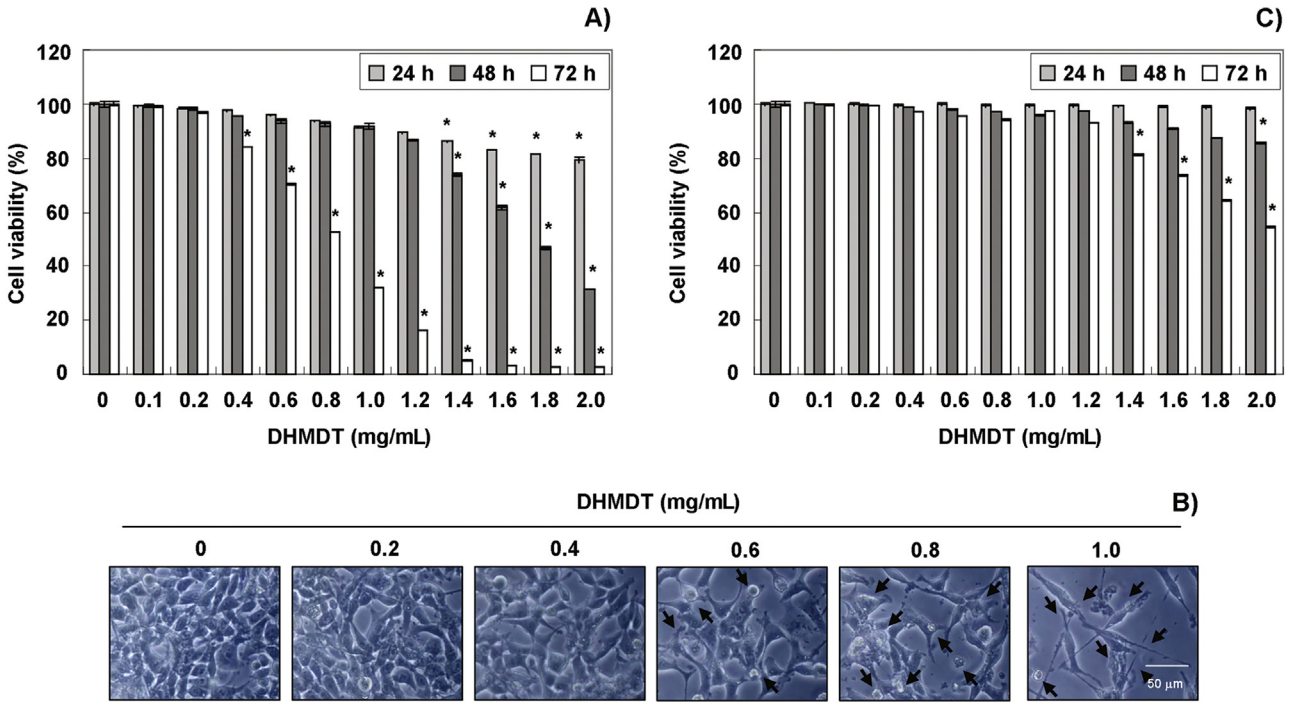

Fig. 1 – Inhibition of cell viability by DHMDT in HCT-116 cells. (A and C) HCT-116 and Chang liver cells were treated with different concentrations of DHMDT for the indicated times. Cell viability was determined by MTT assay. Each point represents the mean ± SD of three independent experiments. The significance was determined by the Student *t* test (*$p < 0.05$ vs. untreated control). (B) The cells were treated with the indicated concentrations of DHMDT for 72 hours and photographed under an inverted microscope; 400 × magnification. DAPI, 4,6-diamidino-2-phenyllindile; DHMDT, Dae-Hwang-Mok-Dan-Tang; MTT, 3-(4,5-dimethyl-2-thiazolyl)-2,5-diphenyl-2H-tetrazolium bromide; SD, standard deviation.

Western blotting showed that DHMDT treatment resulted in a concentration-dependent decrease in the expression levels of XIAP and survivin but not cIAP-1 and cIAP-2 (Fig. 3).

3.4. *DHMDT induced activation of caspases and cleavage of poly(ADP-ribose)-polymerase and phospholipase C-γ1 in HCT-116 cells*

We then examined the expression levels and activities of caspases during DHMDT-induced HCT-116 cell apoptosis. As shown in Fig. 4A, Western blot analyses revealed that the expression levels of pro-caspase-3 in cells treated with DHMDT were concentration-dependently downregulated and the expression levels of active-caspase-3 were upregulated. Moreover, although the active forms of caspase-8 and caspase-9 were not observed, the levels of the proforms of caspase-8 and caspase-9, initiator caspases of extrinsic and intrinsic apoptosis pathways, respectively, were downregulated. Under the same conditions, the *in vitro* activities of the caspases were also measured using colorimetric substrates specific for each caspase, and we found that DHMDT stimulated caspase-3, caspase-8, and caspase-9 activities in a dose-dependent manner (Fig. 4B). In addition, DHMDT treatment led to progressive proteolytic cleavage of poly(ADP-ribose)-polymerase (PARP) and phospholipase C-γ1 (PLC-γ1) proteins (Fig. 4A).

3.5. *DHMDT induced caspase-dependent apoptosis in HCT-116 cells*

To further confirm the involvement of DHMDT-induced activation of caspases, the cells were pretreated with or without Z-VAD-fmk, a pan-caspase inhibitor, for 1 hour, followed by treatment with DHMDT. The results indicated that pretreatment with Z-VAD-fmk resulted in significant prevention of the appearance of cells with apoptotic features, such as chromatin condensation and formation of apoptotic bodies, and attenuation of the progressive accumulation of fragmented DNA following treatment with DHMDT (Fig. 5A and B). Furthermore, z-DEVD-fmk also decreased the accumulation of annexin V-FITC stained cells and increased cell viability in the presence of DHMDT (Fig. 5C and D). These results provide evidence of DHMDT-induced apoptotic cell death in association with activation of caspases in HCT-116 cells.

3.6. *DHMDT truncated Bid and induced the mitochondrial translocation of Bax and the loss of MMP in HCT-116 cells*

To further confirm the DHMDT-induced apoptotic pathway, this study examined the effects of DHMDT on the levels of Bcl-2 family proteins and cytochrome *c*, as well as the MMP values. As shown in Fig. 6A, the total levels of proapoptotic Bax and antiapoptotic Bcl-2 proteins remained unchanged in response

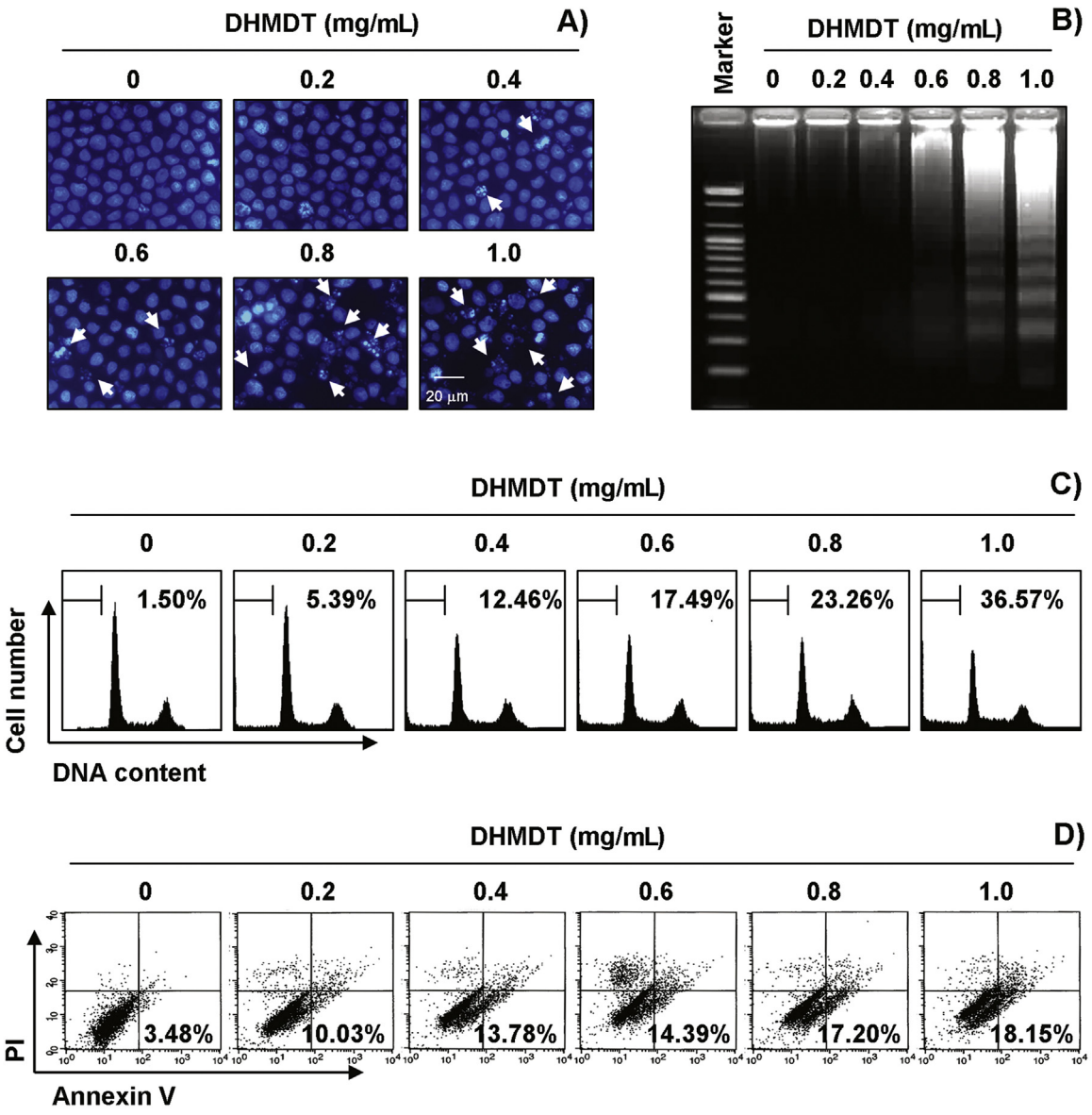

Fig. 2 – Induction of apoptosis by DHMDT in HCT-116 cells. The cells were treated with the indicated concentrations of DHMDT for 72 hours. (A) The nuclei stained with DAPI solution were photographed with a fluorescence microscope using a blue filter; 400 × magnification. (B) For analysis of DNA fragmentation, genomic DNA was extracted, electrophoresed in a 1.5% agarose gel, and visualized by EtBr staining. (C) To quantify the degree of apoptosis induced by DHMDT, the cells were evaluated by a flow cytometer to determine the sub-G1 DNA content. (D) The cells were also stained with annexin V-FITC and PI, and the percentages of the apoptotic cells (annexin V^+ cells) were then analyzed using flow cytometric analysis. (C and D) The data represent the mean of two different experiments. DAPI, 4,6-diamidino-2-phenyllindile; DHMDT, Dae-Hwang-Mok-Dan-Tang; EtBr, ethidium bromide; PI, propidium iodide; V-FITC, V-fluorescein isothiocyanate.

to DHMDT treatment; however, DHMDT treatment decreased the cytosolic levels of Bax, whereas its mitochondrial levels significantly increased after treatment with increasing concentrations of DHMDT (Fig. 6C). Subsequent Western blot analyses revealed progressive downregulation of total Bid protein and accumulation of truncated Bid (tBid) as well as a marked decrease in mitochondrial cytochrome c and a concurrent increase in cytosolic cytochrome c (Fig. 6C). Moreover, DHMDT treatment caused a concentration-dependent loss of MMP in comparison to the untreated control (Fig. 6B). These results suggest that DHMDT inserts Bax from the cytosol into the mitochondria inducing loss of MMP, thereby resulting in mitochondrial dysfunction, release of cytochrome c to the cytosol, and apoptosis induction.

3.7. *DHMDT inactivated the PI3K/Akt pathway in HCT-116 cells*

Because the PI3K/Akt pathway is the most important signaling pathway in both cell growth and in the survival of many

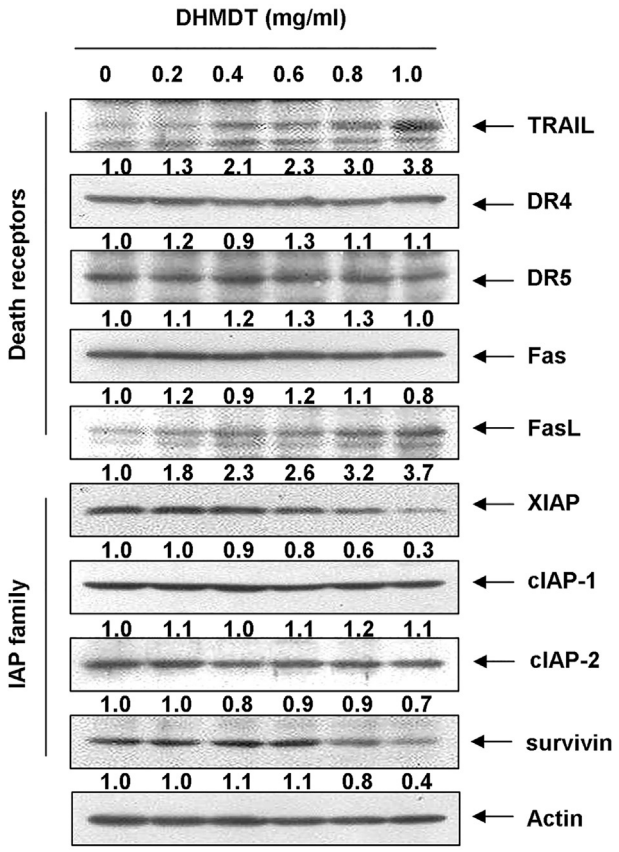

Fig. 3 – Effects of DHMDT on the expression of DR-related and IAP family proteins in HCT-116 cells. The cells were treated with the indicated concentrations of DHMDT for 72 hours. The cells were lysed, and the cellular proteins were visualized using the indicated antibodies and an ECL detection system. Actin was used as an internal control. The relative ratios of expression in the results of Western blotting were presented at the bottom of each of the results as relative values of actin expression. DHMDT, Dae-Hwang-Mok-Dan-Tang; DR, death receptor; ECL, enhanced chemiluminescence; FasL, Fas ligand; IAP, inhibitor of apoptosis protein; TRAIL, tumor necrosis factor (TNF)-related apoptosis-inducing ligand.

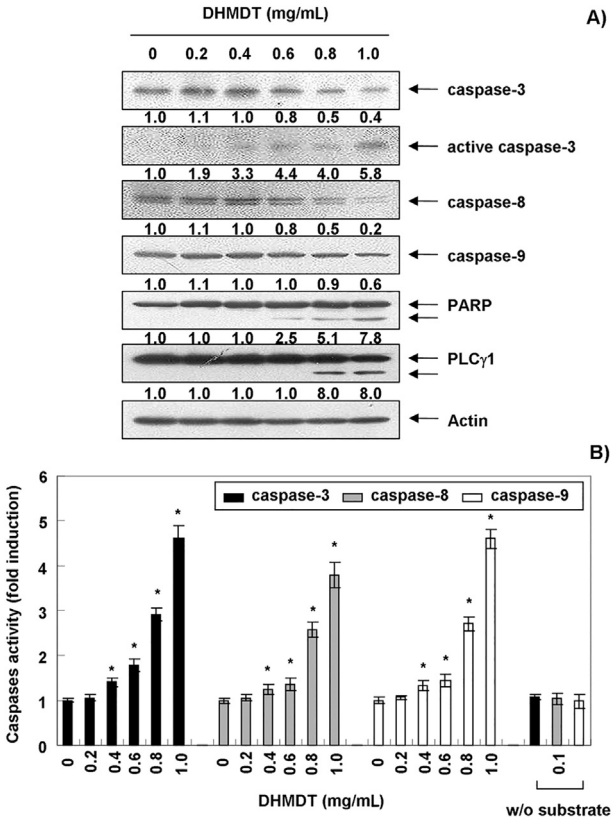

Fig. 4 – Activation of caspases and degradation of PARP and PLC-γ1 by DHMDT in HCT-116 cells. (A) The cells grown under the same conditions as shown in Fig. 3 were lysed, and the cellular proteins were visualized using the indicated antibodies and an ECL detection system. Actin was used as an internal control. The relative ratios of expression in the results of Western blotting were presented at the bottom of each of the results as relative values of actin expression. (B) The cells were lysed, and aliquots (50 μg protein) were assayed for *in vitro* caspase-3, caspase-8, and caspase-9 activities using DEVD-pNA, IETD-pNA, and LEHD-pNA as substrates, respectively, at 37 °C for 1 hour. The released fluorescent products were measured. The data are expressed as the mean ± SD of three independent experiments. The significance was determined using Student *t* test (*$p < 0.05$ vs. untreated control). DHMDT, Dae-Hwang-Mok-Dan-Tang; DR, death receptor; ECL, enhanced chemiluminescence; IETD, Ile-Glu-Thr-Asp; LEHD, Leu-Glu-His-Asp; PLC-γ1, phospholipase C-γ1; pNA, *p*-nitroaniline; PARP, poly(ADP-ribose)-polymerase; SD, standard deviation.

cancers, we determined whether DHMDT-induced apoptosis in HCT-116 cells is involved in this pathway by determining the expression and phosphorylation levels of PI3K and Akt, a downstream effector of PI3K, after treatment with DHMDT. As shown in Fig. 7A, the levels of phosphorylated PI3K and Akt proteins were time-dependently decreased after DHMDT treatment, and they completely disappeared after 48 h; however, the total expression levels of phosphorylated PI3K and the Akt remained the same throughout the experiment. Next, to evaluate the relationship between PI3K/Akt activity and apoptosis, we investigated whether DHMDT significantly induces apoptosis in the presence of LY290042, a specific inhibitor of PI3K. As shown in Fig. 7B–D, treatment of LY294002 markedly increased apoptosis and decreased cell viability in the presence of DHMDT, as demonstrated by nuclear morphology, DNA fragmentation, annexin V-FITC staining, and the MTT assays. Taken together, these results indicate that the PI3K/Akt pathway plays an important role in regulating DHMDT-induced-apoptosis in HCT-116 cells.

4. Discussion

In this study, we investigated whether DHMDT induces apoptosis in HCT-116 cells and sought to identify the mechanisms related to cell death. Our findings demonstrated that

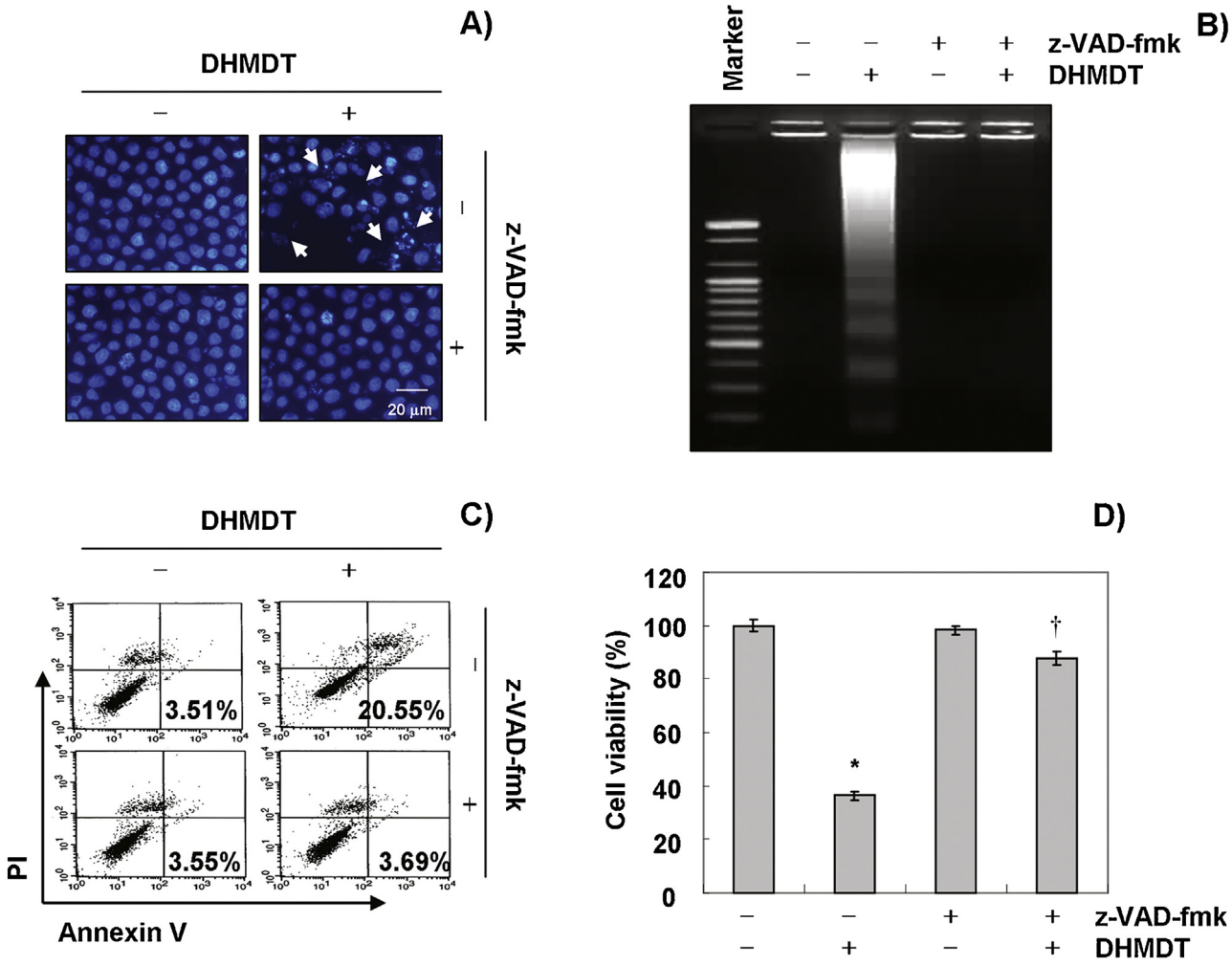

Fig. 5 – Inhibition of DHMDT-induced apoptosis by pan-caspase inhibitor in HCT-116 cells. The cells were pretreated for 1 hour with or without 50 μM Z-VAD-fmk, and then treated with DHMDT for an additional 72 hours. (A) The cells were stained with DAPI and photographed with a fluorescence microscope using a blue filter; 400 × magnification. (B) The genomic DNA from the cells was extracted, separated by electrophoresis in a 1.5% agarose gel, and visualized under UV light after staining with EtBr. (C) The percentages of apoptotic cells (annexin V$^+$ cells) were analyzed using flow cytometric analysis. The data represent the mean of the two different experiments. (D) Cell viability was determined by the MTT assay. Each point represents the mean ± SD of three independent experiments. The significance was determined using Student *t* test (*$p < 0.05$ vs. untreated control; †$p < 0.05$ vs. DHMDT-treated cells). DHMDT, Dae-Hwang-Mok-Dan-Tang; DAPI, 4,6-diamidino-2-phenyllindile; EtBr, ethidium bromide; MTT, 3-(4,5-dimethyl-2-thiazolyl)-2,5-diphenyl-2*H*-tetrazolium bromide; SD, standard deviation; z-VAD-fmk, *N*-benzyloxycarbonyl-Val-Ala-Asp-fluoromethylketone.

DHMDT could time- and concentration-dependently inhibit cell viability and induce apoptosis as measured by chromatin condensation of the nuclei, DNA fragmentation and induction of the sub-G1 phase and annexin V-stained cells, all of which are the hallmark features of apoptosis. It was also suggested that DHMDT stimulates caspase-dependent extrinsic and intrinsic apoptosis pathways in HCT-116 cells. Furthermore, we investigated the linkage between the PI3K/Akt pathway and apoptosis induction, and our results showed that DHMDT increased apoptosis through the inactivation of the PI3K/Akt pathway.

Apoptosis is the rigorous, active, and orderly process of cell death, and dysregulated apoptosis is considered to induce a number of pathological conditions, including cancer. Therefore, the induction of apoptosis is an important target for cancer therapy.[7,8] In the present study, we examined various aspects of the mechanisms of apoptosis induction by DHMDT in human colon cancer HCT-116 cells, and we found that DHMDT activated both initiator caspases (caspase-8 and caspase-9) of the extrinsic and intrinsic pathways, and downstream effector caspase-3 (Fig. 4), which was associated with the degradation of PARP and PLC-γ1; these are hallmarks of apoptosis and substrates of activated caspase.[15,16] Although the levels of DRs, such as DR4, DR5, and Fas, remained unchanged after DHMDT treatment, DHMDT considerably increased the levels of their ligands, including TRAIL and FasL. DHMDT also partially downregulated the IAP family proteins, such as XIAP and survivin, which reportedly block

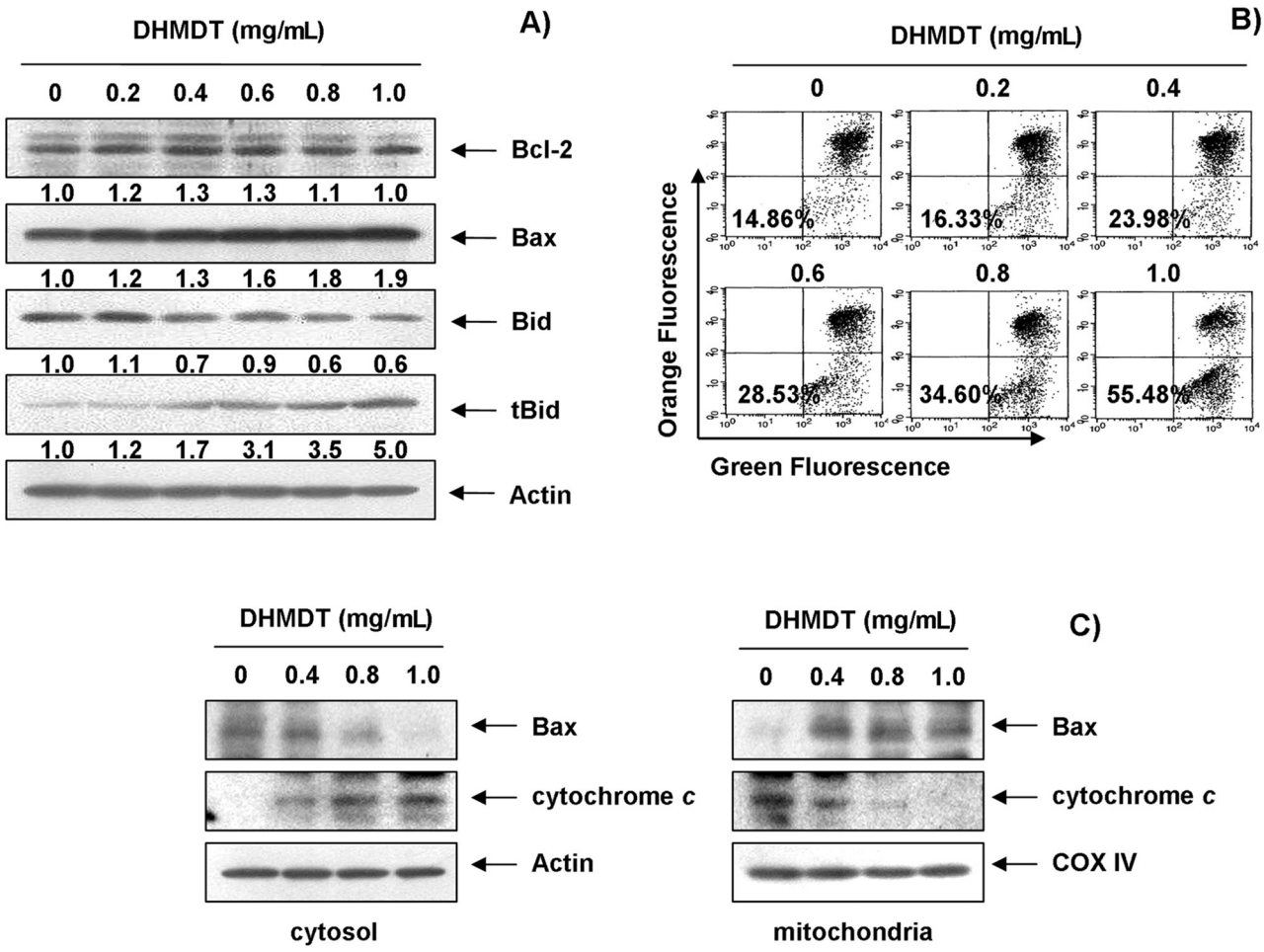

Fig. 6 – Effects of DHMDT on the expression of Bcl-2 family proteins and cytochrome c, and the MMP values in HCT-116 cells. (A) The cells were treated with DHMDT for 72 hours, and the aliquots containing the total protein levels were subjected to SDS-polyacrylamide gels followed by immunoblot analysis with the specific antibodies. The relative ratios of expression in the results of Western blotting were presented at the bottom of each of the results as relative values of actin expression. (B) The cells were collected and incubated with 10 μM JC-1 for 20 minutes at 37 °C in the dark. The cells were then washed once with PBS and analyzed using a flow cytometer. The data is expressed as the mean of two independent experiments. (C) The cytosolic and mitochondrial proteins were extracted from the cells and analyzed by Western blotting using the indicated antibodies. Actin and cytochrome oxidase IV (COX IV) were used as internal controls for the cytosolic and mitochondrial fractions, respectively. DHMDT, Dae-Hwang-Mok-Dan-Tang; MMP, mitochondrial membrane potential; PBS, phosphate-buffered saline; SDS-PAGE, sodium dodecyl sulfate; tBid, truncated Bid.

apoptosis because of their function as direct inhibitors by binding to several caspases and inhibiting them (Fig. 3). However, blocking caspase activity by pretreating the cells with z-DEVD-fmk, a pan-caspase inhibitor, significantly attenuated DHMDT-induced apoptosis and growth inhibition (Fig. 5). Therefore, the data support that DHMDT-induced apoptosis in HCT-116 cells is caspase-dependent, and both the intrinsic and the extrinsic pathways are activated by DHMDT.

In addition, although DHMDT did not affect the total expression levels of proapoptotic Bax or antiapoptotic Bcl-2 in HCT-116 cells, DHMDT treatment resulted in a concentration-dependent increase in the mitochondrial levels of Bax with a concomitant decrease in the cytoplasmic Bax levels. The present data also clearly revealed that DHMDT treatment resulted in a dose-dependent loss of MMP and an increase in the release of cytochrome c from the mitochondria to the cytosol (Fig. 6) with a decline in intact Bid occurring concurrently with a pronounced increase of tBid. Because the release of cytochrome c requires mitochondrial membrane insertion and oligomerization of Bax,[17,18] the translocation of Bax proteins from the cytosol to the mitochondria represents a key event for the activation of the intrinsic pathway. Moreover, caspase-8 connects to the intrinsic pathway via conversion of Bid to form tBid that can translocate to the mitochondrial membrane, where it cooperates with Bax proteins. This cooperation enhances mitochondrial dysfunction, which results in the formation of membrane pores and allows the release of cytochrome c to the cytosol, followed by activation of caspase-9.[17,19] Therefore, our data indicated that DHMDT induces Bid truncation and Bax translocation to the mitochondria from the

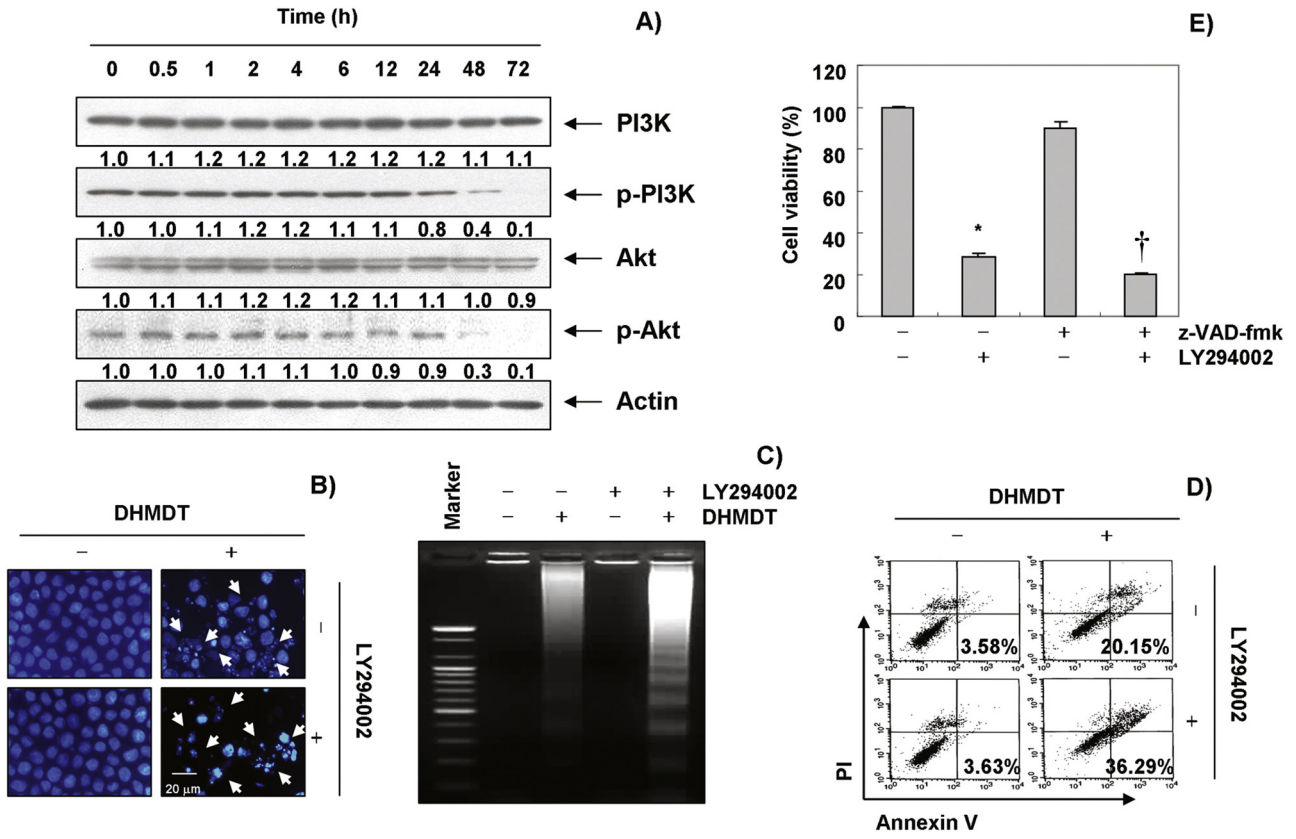

Fig. 7 – DHMDT triggers apoptosis through an inactivation of PI3K/Akt signaling in HCT-116 cells. (A) The cells were treated with DHMDT (1.0 mg/mL) for the indicated times. Equal amounts of cell lysate were resolved by SDS-polyacrylamide gels, transferred to nitrocellulose membranes, and probed with anti-p-PI3K, anti-p-Akt, anti-PI3K, and anti-Akt antibodies. The proteins were visualized using an ECL detection system. Actin was used as an internal control. The relative ratios of expression in the results of Western blotting were presented at the bottom of each of the results as relative values of actin expression. (B–D) The cells were pre-treated with the PI3K inhibitor, LY294002 (50 μM), for 1 hour and then treated with DHMDT (1.0 mg/mL) for 72 hours. (B) After staining with DAPI solution, the nuclei were observed under a fluorescent microscope; 400 × magnification. (C) The genomic DNA from the cells was extracted, separated by agarose gel electrophoresis, and visualized under UV light after staining with EtBr. (D) The percentages of apoptotic cells (annexin V$^+$ cells) were analyzed using flow cytometric analysis. The data is the mean of the two different experiments. (E) Cell viability was determined by the MTT assay. Each point represents the mean ± SD of three independent experiments. The significance was determined using Student *t* test ($^*p < 0.05$ vs. untreated control; $^\dagger p < 0.05$ vs. DHMDT-treated cells). DHMDT, Dae-Hwang-Mok-Dan-Tang; DAPI, 4,6-diamidino-2-phenyllindile; ECL, enhanced chemiluminescence; EtBr, ethidium bromide; PI3K, phosphatidylinositol 3-kinase; SD, standard deviation; SDS, sodium dodecyl sulfate; z-VAD-fmk, N-benzyloxycarbonyl-Val-Ala-Asp-fluoromethylketone.

cytosol, leading to the release of cytochrome *c* by enhancing mitochondrial dysfunction, and finally induction of apoptosis in HCT-116 cells.

By contrast, it was identified that the PI3K/Akt pathway is a well-characterized cell survival signaling pathway, and it blocks apoptosis in a variety of cell types. Notably, the deregulation of the PI3K/Akt pathway is associated with resistance to chemotherapeutic agents,[20,21] and the aberrant activation of this pathway is implicated in the initiation and progression of several types of human malignancies, including lung cancer.[22,23] Therefore, a number of studies have noted that the proapoptotic potential of some anticancer agents is highly correlated with the inactivation of PI3K/Akt pathway,[24–28] indicating that the inhibition of the PI3K/Akt signaling cascade can serve as an effective strategy for the treatment of cancers. Therefore, we further investigated whether the inactivation of the PI3K/Akt pathway is necessary for DHMDT-induced apoptosis, and we found that levels (but not the total levels) of phosphorylated PI3K and Akt were markedly decreased in DHMDT-treated HCT-116 cells (Fig. 7A). In addition, cotreatment with DHMDT and LY294002, a PI3K inhibitor, markedly increased apoptosis and decreased cell viability (Fig. 7B–E), indicating that PI3K/Akt might play a survival role in DHMDT-induced HCT-116 cell apoptosis.

In summary, the results of this study demonstrate that DHMDT triggers apoptosis of human colon cancer HCT-116 cells through activation of the intrinsic caspase pathway along with the DR-mediated extrinsic pathway, and activation of caspases is responsible for the mediation of DHMDT-induced apoptosis. Moreover, the inhibition of the PI3K/Akt pathway

may play an important role in DHMDT-induced apoptosis in HCT-116 cells. Although the results of this study provide new information on the possible mechanisms for the anticancer activity of DHMDT, further studies are needed to identify the active compounds.

Conflicts of interest

The authors declare no conflict of interest.

Acknowledgments

This research was supported by the Basic Science Research Program through the National Research Foundation of Korea (NRF) grant funded by the Korea government (2015R1A2A2A01004633 and 2014R1A1A1008460).

REFERENCES

1. Jemal A, Bray F, Center MM, Ferlay J, Ward E, Forman D. Global cancer statistics. *CA Cancer J Clin* 2011;61:69–90.
2. Cunningham D, Atkin W, Lenz HJ, Lynch HT, Minsky B, Nordlinger B, et al. Colorectal cancer. *Lancet* 2010;375:1030–47.
3. Alberts SR, Wagman LD. Chemotherapy for colorectal cancer liver metastases. *Oncologist* 2008;13:1063–73.
4. Weitz J, Koch M, Debus J, Höhler T, Galle PR, Büchler MW. Colorectal cancer. *Lancet* 2005;365:153–65.
5. Fahy BN, D'Angelica M, DeMatteo RP, Blumgart LH, Weiser MR, Ostrovnaya I, et al. Synchronous hepatic metastases from colon cancer: changing treatment strategies and results of surgical intervention. *Ann Surg Oncol* 2009;16:361–70.
6. Schüller J, Cassidy J, Dumont E, Roos B, Durston S, Banken L, et al. Preferential activation of capecitabine in tumor following oral administration to colorectal cancer patients. *Cancer Chemother Pharmacol* 2000;45:291–7.
7. Fadeel B, Orrenius S. Apoptosis: a basic biological phenomenon with wide-ranging implications in human disease. *J Intern Med* 2005;258:479–517.
8. Sayers TJ. Targeting the extrinsic apoptosis signaling pathway for cancer therapy. *Cancer Immunol Immunother* 2011;60:1173–80.
9. MacKenzie SH, Clark AC. Targeting cell death in tumors by activating caspases. *Curr Cancer Drug Targets* 2008;8:98–109.
10. Brenner D, Mak TW. Mitochondrial cell death effectors. *Curr Opin Cell Biol* 2009;21:871–7.
11. Jin Z, El-Deiry WS. Overview of cell death signaling pathways. *Cancer Biol Ther* 2005;4:139–63.
12. Hensley P, Mishra M, Kyprianou N. Targeting caspases in cancer therapeutics. *Biol Chem* 2013;394:831–43.
13. Lee MH, Lee JW, Park C, Han MH, Hong SH, Choi YH. Antioxidant, antimicrobial and anticancer properties of seven traditional herb-combined remedies. *J Life Sci* 2015;25:406–15.
14. Li Z, Gao Q. Induction of apoptosis in HT-29 cells by quercetin through mitochondria-mediated apoptotic pathway. *Anim Cells Syst* 2013;17:147–53.
15. Kaufmann SH, Desnoyers S, Ottaviano Y, Davidson NE, Poirier GG. Specific proteolytic cleavage of poly(ADP-ribose) polymerase: an early marker of chemotherapy-induced apoptosis. *Cancer Res* 1993;53:3976–85.
16. Bae SS, Perry DK, Oh YS, Choi JH, Galadari SH, Ghayur T, et al. Proteolytic cleavage of phospholipase C-gamma1 during apoptosis in Molt-4 cells. *FASEB J* 2000;14:1083–92.
17. Kadenbach B, Arnold S, Lee I, Hüttemann M. The possible role of cytochrome c oxidase in stress-induced apoptosis and degenerative diseases. *Biochim Biophys Acta* 2004;1655:400–8.
18. Armstrong JS. The role of the mitochondrial permeability transition in cell death. *Mitochondrion* 2006;6:225–34.
19. Lovell JF, Billen LP, Bindner S, Shamas-Din A, Fradin C, Leber B, et al. Membrane binding by tBid initiates an ordered series of events culminating in membrane permeabilization by Bax. *Cell* 2008;135:1074–84.
20. Steelman LS, Stadelman KM, Chappell WH, Horn S, Bäsecke J, Cervello M, et al. Akt as a therapeutic target in cancer. *Expert Opin Ther Targets* 2008;12:1139–65.
21. Heavey S, O'Byrne KJ, Gately K. Strategies for co-targeting the PI3K/AKT/mTOR pathway in NSCLC. *Cancer Treat Rev* 2014;40:445–56.
22. Pal I, Mandal M. PI3K and Akt as molecular targets for cancer therapy: current clinical outcomes. *Acta Pharmacol Sin* 2012;33:1441–58.
23. Silvestris N, Tommasi S, Petriella D, Santini D, Fistola E, Russo A, et al. The dark side of the moon: the PI3K/PTEN/AKT pathway in colorectal carcinoma. *Oncology* 2009;77(Suppl 1):69–74.
24. Tang C, Lu YH, Xie JH, Wang F, Zou JN, Yang JS, et al. Downregulation of survivin and activation of caspase-3 through the PI3K/Akt pathway in ursolic acid-induced HepG2 cell apoptosis. *Anticancer Drugs* 2009;20:249–58.
25. Han MH, Lee WS, Jung JH, Jeong JH, Park C, Kim HJ, et al. Polyphenols isolated from *Allium cepa* L. induces apoptosis by suppressing IAP-1 through inhibiting PI3K/Akt signaling pathways in human leukemic cells. *Food Chem Toxicol* 2013;62:382–9.
26. Lee HW, Jang KS, Chun KH. Celastrol inhibits gastric cancer growth by induction of apoptosis and autophagy. *BMB Rep* 2014;47:697–702.
27. Shin DY, Kim GY, Hwang HJ, Kim WJ, Choi YH. Diallyl trisulfide-induced apoptosis of bladder cancer cells is caspase-dependent and regulated by PI3K/Akt and JNK pathways. *Environ Toxicol Pharmacol* 2014;37:74–83.
28. Yoon J, Ham H, Sung J, Kim Y, Choi Y, Lee JS, et al. Black rice extract protected HepG2 cells from oxidative stress-induced cell death *via* ERK1/2 and Akt activation. *Nutr Res Pract* 2014;8:125–31.